2014 IEEE International Conference on Robotics & Automation (ICRA)
Hong Kong Convention and Exhibition Center
May 31 - June 7, 2014. Hong Kong, China

Modelling of Continuous Dragline Formation in A Mobile Robot

Liyu Wang IEEE & IET Student Member, Cinzia Peruzzi, Utku Culha, Milan Jovic, and Fumiya Iida

***Abstract*— A dragline-forming technology has been previously proposed to enable locomotion through an open-space where no solid surfaces present. The technology is intended for situations where payload requirements are unanticipated. In those situations, variability in dragline's diameter can minimize the use of material hence increase self-sufficiency of the robot. In a previous study, a robot was designed, prototyped and proven to be able to descend through an open-space by forming a thermoplastic dragline with a diameter range of 1.1-4.5 mm. However, the speed of locomotion was rather low due to the lack of an adequate control method for thermoplastic dragline formation. In this paper, models of mass flow and thermodynamics along dragline formation pathway are presented. The models are validated in a newly prototyped robot which forms a dragline continuously. Experiment results show that, when compared to the previous prototype and control method which consists of repeated sequences of discrete events, the speed of descending locomotion is significantly increased and reaches 12.0 cm/min.**

I. INTRODUCTION

Previously a spider-inspired mobile technology has been proposed, where a robot may form draglines from onboard source material to assist its locomotion in an open-space [1]. Compared to climbing technologies, the proposed technology enables mobility through a space where no solid surface presents except the ones at the boundary, e.g. between a ceiling and a ground, or two vertical walls, or two poles, etc. Compared to flying technologies, it could provide a higher payload fraction from dragline assistance. Compared to using an existing cable and a winch [2], [3], it gives variation of dragline thickness, which means that given the same volume of dragline/cable material the length could be adapted without sacrificing the payload need. Hence the proposed technology is suitable for unanticipated task-environments where self-sufficiency is vital. In a previous study, a 300-gram mobile robot has demonstrated descending locomotion from the solid surface of a hanging structure through an open-space without any support other than the dragline formed by itself. The robot was able to form draglines with a diameter range of 1.1-4.5 mm from onboard thermoplastic material, implying a payload range of 0.2-7.7 kg that could be carried [1].

While the demonstration has proven the concept, there remains some technical challenge. One of the biggest challenge is the speed of locomotion being rather low at 0.73 cm/min. That was partially due to the controller being based on repetitions of a sequence of discrete events including supply, deformation and phase transition of the thermoplastic material. It was also because of the choice of design parameters and imprecision in prototyping.

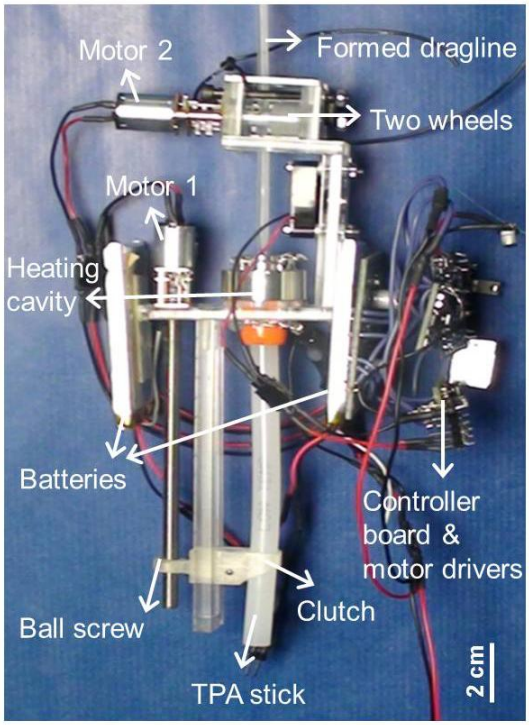

Fig. 1. A dragline-forming mobile robot with onboard material thermoplastic adhesive (TPA). The background surface serves merely for the photographic purpose, not as a support for the robot.

The paper tackles the challenge by showing continuous dragline formation in an improved prototype of the mobile robot. With continuous dragline formation, the sequential events could be carried out in parallel and continuously, and together with mathematical models describing mass flow and thermodynamics, faster locomotion should be achieved. The models are validated in the new prototype which is more precise, lighter and with onboard battery capability. Experiment of descending with continuous dragline formation is carried out to evaluate the performance of the technique.

The remainder of the paper is organized as follows. Section II introduces the newly prototyped dragline-forming mobile robot. Section III describes mathematical models of continuous dragline formation. Section IV presents experimental results of locomotion with continuous dragline formation in a numerical simulation and the physical mobile robot. Section V gives the conclusions of the paper and points

*This work was supported by the Swiss National Science Foundation Professorship Grant No. PP00P2123387/1, and the ETH Zurich Research Grant No. ETH-23-10-3

All authors are with Bio-Inspired Robotics Lab, Department of Mechanical and Process Engineering, ETH Zurich, 8092 Zurich,Switzerland liyu.wang@mavt.ethz.ch

TABLE I

ROBOT SPECIFICATIONS

	Previous prototype [1]	New prototype
Mass	300 g	185 g
Dimension	6×4×18 cm^3	5×3×18 cm^3
DOFs	2	2
Power consumption	2.5 W	4.8-6.8 W
Power source	external	external or onboard

out future work.

II. A DRAGLINE-FORMING MOBILE ROBOT

A robot (see Fig. 1) is prototyped as an improvement from the one reported in [1]. The improved robot weighs ca. 185 gram and has an overall dimension of 5×3×18 cm^3 (width, thickness, height). The mechanical structure of the robot is inspired by the silk production pathway in spiders [4], [5] and mainly consists of two parts i.e. a material extrusion mechanism and a coupled deformation-locomotion mechanism.

The material extrusion mechanism contains solid TPA (GG02, Dremel, USA) in a cylindrical shape (diameter 7 mm length 10 cm). As shown in Fig. 1, the solid TPA stick is linearly delivered through a heating cavity and pushed out of a nozzle. Linear delivery is converted from a DC gear motor's rotation through a ball screw fixed with a TPA stick clutch. The clutch is constrained in linear motion by a linear track, the end of which is rigidly connected with the DC gear motor (motor 1, 250:1 gear ratio, Pololu, USA) and the heating cavity. The heating cavity lies in a cylindrical aluminium block and has an opening of 7 mm in diameter at one end and a nozzle with an inner diameter of 4 mm and an outer diameter of 6 mm at the other end. The cavity is heated by six 10-Ω power resistors connected in parallel and inserted in the block around the cavity. The TPA stick is held by the clutch at one end and inserted into the aluminium cavity at the other end through a silicone tube for leakage prevention.

The deformation-locomotion mechanism consists of two geometrically identical cylindrical wheels with a diameter of 12 mm, which are contained in a box. One of the wheels is fixed on the output shaft of a second DC gear motor (motor 2, 1000:1 gear ratio, Pololu, USA), and the shaft is fixed on two opposite walls of the containing box. The second wheel is attached around a second shaft which can move linearly on a track with a fixed length on the two walls. The end points of the latter wheel's shaft are attached to the box with springs, which pull the wheel towards the centre of the mechanism. The track constraints this wheel to move along a linear route while springs allow it to passively adjust to the variable diameter of the formed dragline. The spring force is in a linear relation with the distance between the two wheels, or in other words with the diameter of the formed dragline. The force gives the normal force which generates the friction between the formed dragline and the wheels, enabling the robot to hold onto the formed dragline when being static. During movement, the mechanism enables the robot to elongate extruded material as well as moving along a formed dragline.

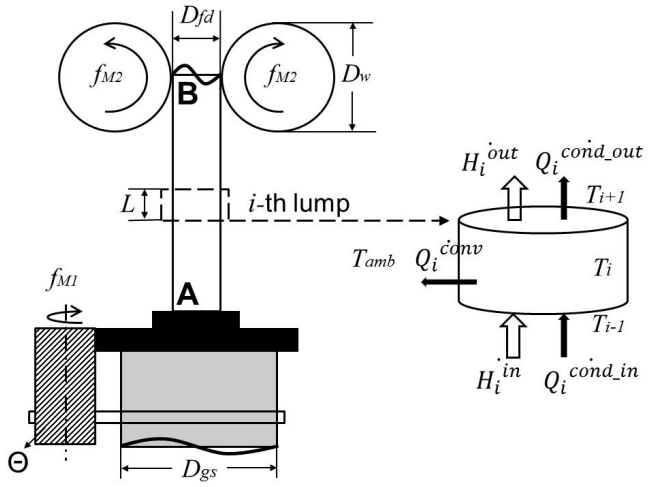

Fig. 2. Illustration of thermoplastic dragline formation pathway. Lumped parameter method is used to model the process of continuous dragline formation. Each thermal reservoir is a lump and modelled as a thermodynamic open system (the i-th thermal reservoir is shown). The mass reservoir is virtually and geometrically overlapped with the first lump above the nozzle (point A).

The two parts are arranged in such a way that the deformation-locomotion mechanism is on the upper body of the robot, and the material extrusion mechanism is on the lower body. They are connected by a rigid piece so that the exit of the extrusion nozzle is placed at a distance of 4 cm under the bottom of the deformation-locomotion mechanism. A fan is attached to the connecting piece so that forced convection for cooling is possible when needed. An electronics unit includes two motor drivers (Dual MC33926, Pololu, USA), a microcontroller board (Arduino Pro Mini, Italy), and a USB adapter. The robot could be powered by external power source, or by two Lithium-Polymer batteries (ICP543759PMT, Renata, Switzerland). A summary of the robot and its comparison to the previous prototype is detailed in Table I.

III. MATHEMATICAL MODELS FOR CONTINUOUS DRAGLINE FORMATION

To realize continuous dragline formation, the material flow and thermodynamics of the dragline forming process needs to be carefully modelled. On the one hand, the material inflow rate and outflow rate determine the thickness of a dragline segment and hence its surface areas, which will have an effect on thermodynamics. On the other hand, thermodynamics determines cooling which sets constraints on the highest possible temperature of a dragline segment before it gets grabbed by the robot as a support. Since the system couples locomotion with deformation, the constraints also have an effect on the speed of the motor for locomotion hence the material outflow rate.

To model the mass flow of material and thermodynamics of the dragline formation process, lumped capacitance

method [6] is used because it is simple, sufficient and computationally inexpensive for numerical simulation. Specifically, by denoting the distance between the exit of the nozzle (point A in Fig. 2) and the middle contact point on the wheels (point B) as L_{AB}, the dragline between the nozzle and the two wheels can be represented by N lumps. That means the lumps are fixed relative to the robot. All lumps have the same length along the axis of the dragline, therefore the length of each lump is $L = L_{AB}/N$. In this section, the mass flow model and the thermodynamics model are described.

A. Mass Flow Model

Mass flow is modelled with the inflow and outflow of material within a certain reservoir that is geometrically overlapped with the very first lump just above the nozzle. It is assumed that the dragline after the mass reservoir has a constant crosssection diameter D_{fd}. At a certain time t, the mass flow $m(t)$ through the sole mass reservoir is the integral of mass flow rate over time:

$$m(t) = \int_0^t \dot{m}(t) \cdot dt \tag{1}$$

where the mass flow rate $\dot{m}$ depends on the mass inflow and outflow rates:

$$\dot{m}(t) = \dot{m^{in}}(t) - \dot{m^{out}}(t) \tag{2}$$

With the robot design introduced in Section II, the inflow rate and outflow rate are related to the extrusion mechanism and locomotion-deformation mechanism respectively:

$$\dot{m^{in}}(t) = \rho\pi\frac{{D_{gs}}^2}{4}\Theta \cdot f_{M1}(t) \tag{3}$$

$$\dot{m^{out}}(t) = \rho\pi\frac{D_{fd}(t)^2}{4}\pi D_w \cdot f_{M2}(t) \tag{4}$$

where ρ is the density of the TPA, D_{gs} is the crosssection diameter of the solid TPA stick, Θ is the pitch of the single-start ball screw, D_{fd} is the crosssection diameter of the formed dragline that leaves the wheels, D_w is the diameter of the two wheels, f_{M1} is the number of revolutions per second (rps) of motor 1 and f_{M2} is the number of revolutions per second of motor 2.

The crosssection diameter of the dragline at time $t + dt$ is a result of the mass flow in the mass reservoir at time t:

$$D_{fd}(t + dt) = 2\sqrt{\frac{m(t)}{\rho\pi L}} \tag{5}$$

B. Thermodynamics Model

Each lump is a thermal reservoir which is a thermodynamic open system [7]. By assuming no flow work or shaft work and a single temperature for each thermal reservoir, as shown in Fig. 2 for the i-th reservoir from the nozzle (i=1,2,...,N), its change in internal energy obeys the first law of thermodynamics, and the changing rate of the internal energy at a certain time t is:

$$\dot{U}_i(t) = c \cdot m_i(t) \cdot \dot{T}_i(t) = \dot{Q}_i(t) + \dot{H_i^{in}}(t) - \dot{H_i^{out}}(t) \tag{6}$$

TABLE II
PARAMETER VALUES FOR MODELS

Distance between nozzle and wheels L_{AB}	0.04 m
Pitch of the single-start ball screw Θ	0.001 m
Diameter of the wheels D_w	0.012 m
Diameter of solid TPA stick D_{gs}	0.007 m
Density of TPA ρ	1.0×10^3 kg/m^3
Specific heat capacity of TPA c	2500 J/(kg·°C)
Thermal conductivity of TPA K	0.45 W/(m·°C)
Heat transfer coefficient of air h	30 W/(m^2·°C)
Bond formation temperature of TPA T_{bf}	50°C
Temperature of extrusion T_{extru}	70°C
Ambient temperature T_{amb}	25°C

where c is specific heat capacity of the TPA, $\dot{T}_i(t)$ is the changing rate of temperature within that thermal reservoir at t, and $m_i(t)$ is the mass of that thermal reservoir at t:

$$m_i(t) = \rho A_i^{cond}(t)L$$

The right side of (6) indicates that the changing rate of the energy into and out of the system is due to two factors, i.e. heating and mass flow. The changing rate of the energy due to heating is:

$$\dot{Q}_i(t) = \dot{Q_i^{cond\_in}}(t) - \dot{Q_i^{cond\_out}}(t) - \dot{Q_i^{conv}}(t) \tag{7}$$

where it is caused by conduction into and out of the system and convection out of the system. Conduction could be modelled with Fourier's law and convection could be modelled with Newton's cooling law:

$$\dot{Q_i^{cond\_in}}(t) = \frac{K \cdot A_i^{cond}(t)}{L} \cdot (T_{i-1}(t) - T_i(t)) \tag{8}$$

$$\dot{Q_i^{cond\_out}}(t) = \frac{K \cdot A_i^{cond}(t)}{L} \cdot (T_i(t) - T_{i+1}(t)) \tag{9}$$

$$\dot{Q_i^{conv}}(t) = h \cdot A_i^{conv}(t) \cdot (T_i(t) - T_{amb}) \tag{10}$$

in which K is the thermal conductivity of the TPA, h is the heat transfer coefficient between the TPA and the environment, and the surface area related to conduction is the crosssection of the dragline and the surface area related to convection is the surrounding of the dragline:

$$A_i^{cond}(t) = \frac{\pi \cdot D_{fd}(t)^2}{4}$$

$$A_i^{conv}(t) = \pi \cdot D_{fd}(t) \cdot L$$

The changing rate of the energy into and out of the system due to the mass flow is:

$$\dot{H_i^{in}}(t) = c \cdot \dot{m}(t - (i-1) * \tau) \cdot T_{i-1}(t) \tag{11}$$

$$\dot{H_i^{out}}(t) = c \cdot \dot{m}(t - (i-1) * \tau) \cdot T_i(t) \tag{12}$$

Here τ is a unit delay factor caused by the mass flow through each lump. As mentioned in subsection III.A, the mass reservoir is geometrically overlapped with the first lump above the nozzle, thus the mass flow through each lump is delayed according to the lump ID from the nozzle. τ is determined as:

$$\tau = \frac{L}{\pi \cdot D_w \cdot f_{M2}(t)} \tag{13}$$

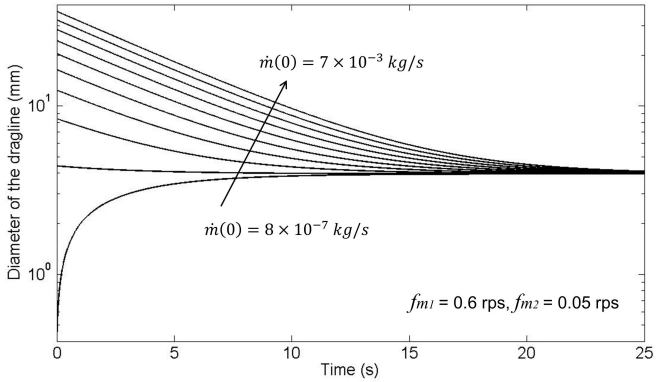

Fig. 3. Simulation result showing that dragline diameter at the equilibrium state is independent from initial conditions.

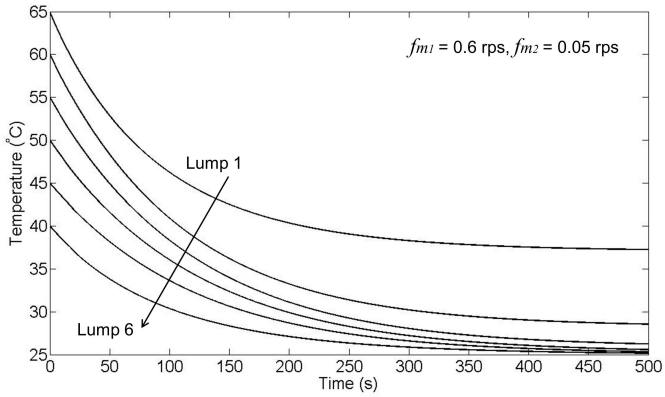

Fig. 4. Simulation result showing thermodynamics of all lumps.

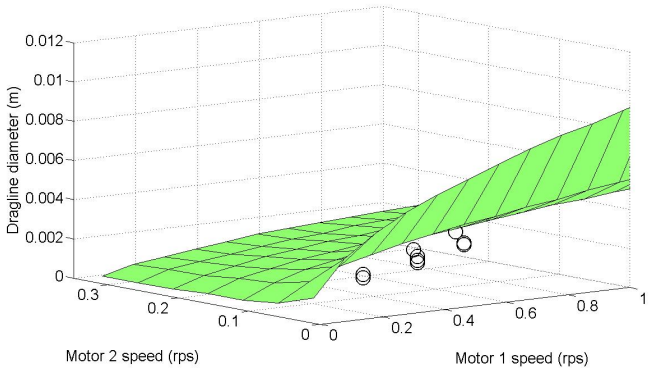

Fig. 5. Experiment results from simulation (surface) and real world (circle markers) showing dragline diameter at the equilibrium state under various constant motor speeds.

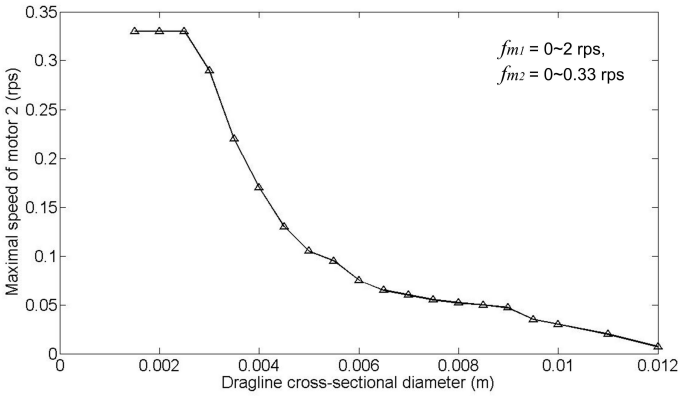

Fig. 6. Simulation result showing that maximal locomotion speed (speed of motor 2) depends on the target dragline diameter.

The thermodynamics model is subject to boundary conditions for temperatures at the two ends between L_{AB}:

$$T_0 = T_A = T_{extru}$$

$$T_{N+1} = T_B = T_{amb}$$

where T_{extru} is the temperature of TPA inside the heating cavity, and T_{amb} is the ambient temperature.

IV. EXPERIMENT AND RESULTS

To validate the above models and evaluate the performance of continuous dragline formation, simulation and real-world experiments have been carried out. Specifically, the following aspects were looked into: the diameter range, the locomotion speed, and the repeatability of a dragline.

A. Simulation

To systematically study the relation between constant motor speed and dragline diameter, numerical simulation was implemented in Matlab Simulink based on the above two mathematical models. In the simulation, design parameters of the robot and realistic physical parameters of the TPA and the environment were used (see Table II). More specifically, six lumps were constructed (N=6). The speeds of the two motors f_{M1} and f_{M2} were set for different values but constant over each run. Various initial conditions of mass flow rate $\dot{m}(0)$ and temperature of each lump $T_i(0)$ were simulated. The simulation under each conditions was run for 500 seconds with variable time steps.

Fig. 3 shows the change of the diameter of a dragline over time during simulation with motor speed f_{M1}=0.6 rps and f_{M2}=0.05 rps. The diameter of a dragline reaches an equilibrium state after some time, and that is because the mass flow in (5) has stabilized. Simulation with various initial conditions of mass flow rate from 8×10^{-7} kg/s to 7×10^{-3} kg/s indicates that the diameter of the dragline at the equilibrium state does not depend on the initial conditions.

Fig. 4 shows the thermodynamics of all the lumps during simulation with motor speed f_{M1}=0.6 rps and f_{M2}=0.05 rps. From an initial temperature that is higher than T_{amb}, each lump decreases temperature until an equilibrium state has been reached. The important lump here is lump 6, which is the lump just below the two wheels where the dragline is grabbed. The criteria for a successful formation requires that the temperature of lump 6 should be below bond formation temperature T_{bf} [8], under which TPA is no longer adhesive thus it won't stick onto the wheels. It is assumed here this criteria is always reached in the thermodynamics model and simulation.

Fig. 5 shows the simulation result for a range of

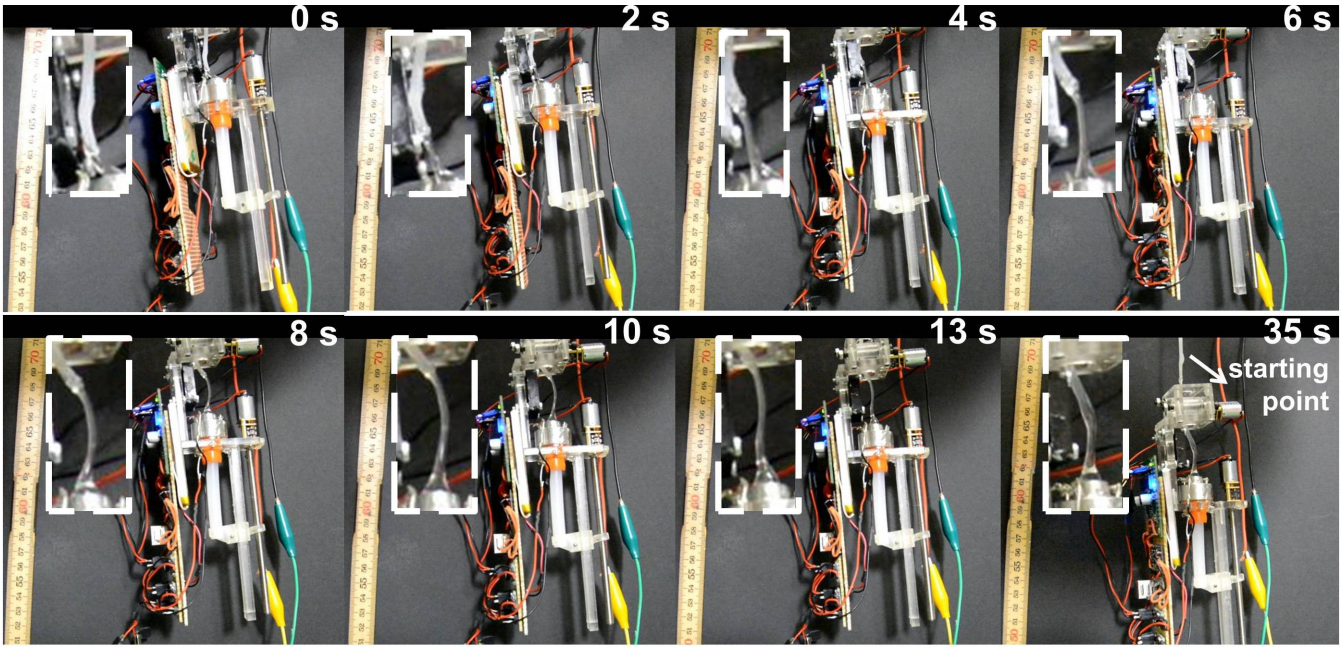

Fig. 7. Snapshots of a trial in the real-world experiment, where motor 1 was given a signal of a 100% duty cycle and motor 2 a 30% duty cycle (trial ID 5 in Fig. 8). In the last snapshot the starting point is indicated to show the robot moved stably on the dragline formed by itself. Insets, magnified view of dragline segments being formed.

motor speeds with initial conditions $\dot{m}(0)=8.38\times10^{-5}$ kg/s, $T_1(0)=65°C$, $T_1(0)=60°C$, $T_1(0)=55°C$, $T_1(0)=50°C$, $T_1(0)=45°C$,$T_1(0)=40°C$. The result indicates that the higher the constant speed of motor 1 and the lower the constant speed of motor 2 is, the thicker the dragline at the equilibrium state will be. Quantitatively, the result can be fitted into a polynomial function with a Sum-of-Squares-Due-to-Error of 3.412×10^{-5}:

$$D_{fd} = 0.004598 + 0.005114 \cdot f_{M1} - 0.0728 \cdot f_{M2}$$

$$-0.0338 \cdot f_{M1} \cdot f_{M2} + 0.4337 \cdot {f_{M2}}^2$$

$$+0.06996 \cdot f_{M1} \cdot {f_{M2}}^2 - 0.7781 \cdot {f_{M2}}^3$$

It is worth mentioning that, significantly different initial conditions have been simulated and no change in the above relation has been found.

It can be also seen from the above relation that, given a target D_{fd}, the speed of motor 1 can be adjusted such that the speed of motor 2 is the highest possible at that target D_{fd}. That is important to find the maximal locomotion speed of the robot. Interestingly, the maximal locomotion speed (derived from that of motor 2) depends on D_{fd}. As shown by the theoretical result in Fig. 6, given a range of possible motor speeds (in this case f_{M1} 0-2 rps and f_{M2} 0-0.33 rps), the maximal locomotion speed decreases with the increase of target dragline diameter. This feature did not present in the previous dragline forming method that was based on discrete events [1], and it is due to coupling between mass flow and thermodynamics in continuous dragline formation.

B. Real-World Experiment

Real-world experiment of vertical descending was conducted with the physical robot. The robot started by holding onto the lower tip of a TPA string with a diameter of 2 mm clamped at a height. The robot was externally powered with 6.8 W so that the TPA extrusion temperature could be maintained at 70°C. The two DC motors were controlled by PWM signals in different duty cycles in a pre-programmed feed-forward controller. Specifically, twelve trials were made under different conditions of motor speed, where the duty cycles for motor 1 ranged 50%-100% corresponding to a speed from 0.3 to 0.6 rps and for motor 2 ranged 25%-30% corresponding to a speed from 0.05 to 0.07 rps (less duty cycle resulted in a too low voltage to drive motor 2).

The robot succeeded in holding onto the dragline formed by itself and descending with it in ten trials. The diameter of resulting draglines was between 1.2 mm and 3.2 mm (mean of ten sampling locations along each dragline), and the maximal length of the draglines was 66 cm. Fig. 7 shows snapshots of the first 35 seconds in one of the trials (Trial ID 5, also see a multimedia video). In the trial, motor 1 was given a signal of a 100% duty cycle (0.6 rps) and motor 2 a 30% duty cycle (0.07 rps). As a result, a dragline with a mean diameter of 3.1 mm was formed and it reached 36 cm until the solid TPA stick had to be manually replaced. It can be seen from the figure that the robot descended 7 cm in 35 seconds, indicating a locomotion speed of 12.0 cm/min, which is 16 times as fast as the speed reported in [1].

Fig. 5 plots the dragline diameters of the ten trials, indicated by circle markers. It can be seen that the diameters of the formed draglines are slightly smaller than the simulation

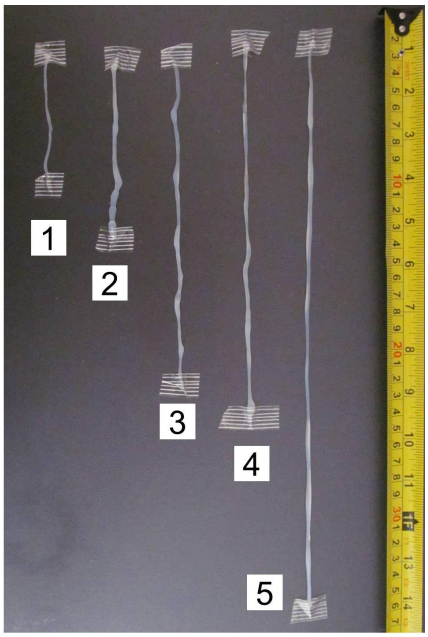

Fig. 8. Dragline samples from five of the trials from the real-world experiment.

TABLE III
PERFORMANCE OF DRAGLINE FORMATION

	Discrete formation with previous prototype [1]	Continuous formation with new prototype
Dragline diameter	1.1-4.5 mm	1.2-3.2 mm
Dragline length	10 cm	66 cm
Repeatability	10-25%	5-20%
Maximal speed	0.73 cm/min	12.0 cm/min

results. That is probably due to the fact that TPA accumulated in an irregular shape after being extruded at the exit of the nozzle, as shown in the insets in Fig. 7. The cone shape made the dragline thinner than the one if TPA were accumulated in a cuboid shape.

Regarding the repeatability of dragline formation, which was measured in relative deviation between dragline diameters and predicted values, the relative deviation using continuous dragline formation is 5-20% which has improved from the method previously used. The reason of improvement is that the motors did not have to stop and start from time to time but rather operated continuously. Fig. 8 shows the resulting draglines from five of the successful trials, which further visualizes the fairly consistent profile of formed draglines. Failure occured in two out of the twelve trials in which initial TPA supply was not stable resulting too thin a segment of the dragline.

A summary about the performance of continuous dragline formation from the experiment with the physical robot is given in Table III.

V. CONCLUSIONS AND FUTURE WORK

The paper presents modelling of continuous dragline formation based on thermoplastics material for the use of a mobile technology in an open-space with unanticipated payload requirements. Mathematical models are established on mass flow of thermoplastics source material and thermodynamics along the dragline formation pathway. Numerical simulation has been conducted based on the models, and a physical robot containing TPA has been constructed with improvement over the previous prototype. Simulation results suggest the theoretical relation between motor speeds and dragline diameter, and that maximal locomotion speed is inversely correlated to the target dragline diameter. Real-world descending experiment results validate the models and show that the 185-gram robot could move 16 times as fast as with the old prototype and discrete control method previously proposed, reaching 12.0 cm/min. It is worth mentioning that, a recent study [9] using the new prototype and the previous control method also confirms the contribution of continuous dragline formation in doubling the locomotion speed.

Future work includes studying other methods to further increase the locomotion speed and improve the repeatability for practical applications. There are at least three possible ways to further increase the locomotion speed. Firstly, design parameters such as the distance between the wheels and the nozzle could be made larger. Secondly, better active cooling method than a fan can be implemented to increase the heat transfer coefficient. Thirdly, other types of TPA with a lower softening point may be helpful. Other interesting scientific questions worth investigation are related to the exploration of other types of thermoplastics as well as the initialization of the dragline formation from a solid structure. For example, questions such as how stronger thermoplastics affects the speed and power consumption, or how adhesion with the boundary surfaces affects repeatability of a dragline, could also widen the applications of the technology.

REFERENCES

[1] L. Wang, U. Culha, and F. Iida “Free space locomotion with thread formation,” in Proc. 2013 IEEE/RSJ Int. Conf. Robotics and Intelligent Systems, Tokyo, pp. 4046-4051.
[2] M. Bonani, S. Magnenat, P. Retornaz, and F. Mondada, “The Hand-Bot, a robot design for simultaneous climbing and manipulation,” in Proc. 2nd Int. Conf. Intelligent Robotics and Applications, Singapore, 2009, pp. 11-22.
[3] A. Capua, A. Shapiro, and S. Shoval, “SpiderBot: A cable suspended mobile robot,” in Proc. 2011 IEEE Int. Conf. Robotics and Automation, Shanghai, 2011, pp. 3437-3438.
[4] R. S. Wilson, “The control of dragline spinning in the garden spider,” Quart. J. Micr. Sci., vol. 104, 1962, pp. 557-571.
[5] F. Vollrath and D. P. Knight, “Liquid crystalline spinning of spider silk,” Nature, vol. 410, 2001, pp. 541-548.
[6] T. L. Bergman, A. S. Lavine, F. P. Incropera, and D. P. Dewitt, Fundamentals of Heat and Mass Transfer (7th Ed). John Wiley and Sons, Inc., 2011, ch. 5.
[7] Rules of Thumb for Mechanical Engineers, J. E. Pope Eds. Houston: Gulf Professional Publishing, 1997, pp. 58-59.
[8] Adhesives and Adhesive Tapes, G. Gierenz and W. Karmann, Eds. Weinheim: Wiley-VCH Verlag GmbH, 2001, p. 20.
[9] L. Wang, U. Culha, and F. Iida, “A dragline-forming mobile robot inspired by spiders,” Bioinspir. Biomim., vol. 9, 2014, pp. 016006.